plants

MDPI

Article

Romanian *Viscum album* L.—Untargeted Low-Molecular Metabolomic Approach to Engineered Viscum–AuNPs Carrier Assembly

Adina-Elena Segneanu [1], Catalin Nicolae Marin [2,*], Dumitru Daniel Herea [3], Ionut Stanusoiu [4], Cornelia Muntean [4] and Ioan Grozescu [4]

[1] Institute for Advanced Environmental Research-West, University of Timisoara (ICAM-WUT), Oituz nr. 4, 300086 Timisoara, Romania; adina.segneanu@e-uvt.ro
[2] Faculty of Physics, West University of Timisoara, 300223 Timisoara, Romania
[3] National Institute of Research and Development for Technical Physics, 47 Mangeron Blvd, 700050 Iasi, Romania; dherea@phys-iasi.ro
[4] CAICON Department, University Politehnica Timisoara, 300006 Timisoara, Romania; stanusoiu@gmail.com (I.S.); cornelia.muntean@yahoo.com (C.M.); ioangrozescu@gmail.com (I.G.)
* Correspondence: catalin.marin@e-uvt.ro

Abstract: Viscum is one of the most famous and appreciated medicinal plants in Europe and beyond. The symbiotic relationship with the host tree and various endogenous and ecological aspects are the main factors on which the viscum metabolites' profiles depend. In addition, European traditional medicine mentions that only in two periods of the year (summer solstice and winter solstice) the therapeutic potential of the plant is at its maximum. Many studies have investigated the phytotherapeutic properties of viscum grown on different species of trees. However, studies on Romanian viscum are relatively few and refer mainly to the antioxidant and antiproliferative activity of mistletoe grown on *Acer campestre*, *Fraxinus excelsior*, *Populus nigra*, *Malus domestica*, or *Robinia pseudoacacia*. This study reports the first complete low-molecular-weight metabolite profile of Romanian wild-grown European viscum. A total of 140 metabolites were identified under mass spectra (MS) positive mode from 15 secondary metabolite categories: flavonoids, amino acids and peptides, terpenoids, phenolic acids, fatty acids, organic acids, nucleosides, alcohols and esters, amines, coumarins, alkaloids, lignans, steroids, aldehydes, and miscellaneous. In addition, the biological activity of each class of metabolite is discussed. The development of a simple and selective phyto-engineered AuNPs carrier assembly is reported and an evaluation of the nanocarrier system's morpho-structure is performed, to capitalize on the beneficial properties of viscum and AuNPs.

Keywords: low-weight metabolites; viscum; mass spectra; bioactive compounds; phyto-engineered gold nanoparticles carrier assembly

Citation: Segneanu, A.-E.; Marin, C.N.; Herea, D.D.; Stanusoiu, I.; Muntean, C.; Grozescu, I. Romanian *Viscum album* L.—Untargeted Low-Molecular Metabolomic Approach to Engineered Viscum–AuNPs Carrier Assembly. *Plants* **2022**, *11*, 1820. https://doi.org/10.3390/plants11141820

Academic Editor: Suresh Awale

Received: 9 June 2022
Accepted: 6 July 2022
Published: 11 July 2022

1. Introduction

Since ancient times, viscum was the "crown jewel" of European traditional medicine. Viscum is considered the universal healing plant, to which have been attributed to many symbols and rituals throughout the world. Practically all over the world, there are many superstitions, ceremonials, and legends associated with the mistletoe that grows on a specific host tree [1–5]. For instance, in Europe, a viscum-grown oak tree is said to have mystical properties (banishing witches and evil spirits, battle protection, finding treasures, love, fecundity, and so on) [1–5].

For the Druids, viscum was a divine tree, which grows without roots. It was evergreen, which is why it represents a connection between heaven and earth; the source of life for the tree's spirit.

In Japan, Ainu attributed properties similar to the viscum-grown willow tree [1–5]. There were rituals related to the manner and period of the viscum harvest all over Europe.

The Druids considered that summer solstice was the moment when the maximum potential of the plant was reached. However, in many northern European countries, viscum was harvested during the winter and was associated with love, peace, protection, and fertility.

Later, in Christian Europe, the tradition of viscum was perpetuated. Nowadays, between Christmas and New Year, the houses are decorated with viscum twigs, as a symbol of eternal life, protection, and fortune [1–3].

Viscum's healing properties have been well known since ancient times. The famous scholars Hippocrates, Pliny the Elder, and then Paracelsus and Hildegard of Bingen used the plant for various diseases of the spine, liver, infertility, epilepsy, and ulcers [6].

Afterwards, viscum was considered a remedy for pain, parotitis, epilepsy, edema, cardiac diseases, and hepatitis [6]. At the beginning of the 20th century, in Europe, the hypertensive and antitumor activity of the plant was studied [6]. However, viscum's therapeutic properties (antidiabetic, analgesic, anti-inflammatory, and hypotensive) were already known in Asian (Israel, China, India and Japan) and African traditional medicine [6,7].

Currently, viscum is used as a complementary treatment in cancer therapy in several European countries, where there are different types of commercial phytotherapeutic extracts: Iscador, Isorel, Eurixor, Plenesol, Vysorel, Lektinol, Helixor, Cefalektin, and Lektinol [4–7]. Some studies report also that its extract enhances an organism's immune response [4]. However, the phytotherapeutic effects of medicinal plants and their use in the therapy of severe conditions, such as cancer or neurodegenerative diseases, is still a contradictory topic in Western medicine [8,9].

The highly complex chemical composition and biological activity of viscum could be the result of a mixture of biotic (mainly host tree) and abiotic characteristics (water quantity, soil, pH, temperature, sun exposure, harvest season, and growth stage of the plant) [10,11].

Various research reported a large number of phytochemicals, such as lectins (glycopeptides), viscotoxins, terpenoids, coumarins, flavonoids, peptides, carbohydrates, sterols, alkaloids, proteins, amines, polyphenols, amino acids, and lignans [6–12]. These compounds were studied extensively to establish a relationship between antitumor activity and their biological properties. The main molecules in viscum considered to pose antitumor properties are lectins and viscotoxins. However, recent studies have reported that other secondary metabolites, such as triterpenoids and phenolic derivatives, have anticancer properties [6,7]. It has also been found that the antitumor activity of particular metabolites isolated from viscum is much lower than that of the extract itself. It is due to the synergistic action by which metabolites act [6–13].

Latest studies have shown that viscum extract has positive effects on the quality of life of cancer patients by reducing the side effects of chemo and radiation therapy [14–16]. However, the results of the studies indicate that the antitumor activity of viscum seems to be influenced by several factors (the amount of plant used in the extract, the type of host tree, and the harvest period).

Studies have shown the existence of variation in the content of lectins and viscotoxins depending on the season. Thus, there is a maximum of these phytoconstituents in the viscum samples collected in June and December, thus confirming the practices of traditional medicine [17]. Although various recent research reported the cytotoxic, apoptotic, anti-inflammatory, and immunological effects of viscum, the antitumor mechanism is not fully elucidated and not fully understood [15,16].

Gold has influenced human civilization from the humanity dawn through its characteristics and availability, both materially (social hierarchy) and spiritually. From an esoteric and religious point of view, it was considered a symbol of perfection, immortality, rejuvenation, health, and wisdom. In human belief, gold played an essential role: from the symbolism of the sun in astrology to the highest degree of development of matter (mind, spirit, and soul) in alchemy, as well as the renewal and regeneration of humanity to perfection, enlightenment, and spiritual elevation. In Christianity, gold was associated with divine worship and love [18,19].

In medicine, gold has been used for medical purposes since ancient times. In traditional Chinese medicine, gold was used as a therapeutic agent for various ailments (joint, lungs, measles, skin ulcers, wounds, seizures, detoxification, palpitation, coughing, typhoid fever, and so forth) [20]. In Indian traditional medicine (Ayurveda and Siddha), gold is also used for infertility, asthma, diabetes, and cancer [21]. The Ayurvedic gold preparations are a mixture of gold nanoparticles and herbs used, in which the metal had a double role as a carrier and therapeutic agent [22,23].

Since antiquity there has been evidence of the use of gold in traditional European medicine, such as for skin infection treatment and as an antidote to mercury poisoning [24]. Archaeological discoveries show that in ancient Egypt it was used for dental work [25,26].

Later, in the Middle Ages, according to the documents of the time, "*aurum potabile*" or other gold-based preparations were used for many types of heart conditions, digestive ailments, baldness, fever, and so on [26,27].

Since the end of the 19th century, gold therapy has been adopted for the treatment of syphilis, tuberculosis, rheumatoid arthritis, and other types of arthritis. Scientific results have shown the ineffectiveness of gold derivatives in treating tuberculosis. It is noteworthy that chrysotherapy (or therapy with gold compounds) is accepted and implemented in modern medicine for rheumatoid arthritis treatment. Gold compounds have demonstrated anti-inflammatory properties and are used as a common medication for chronic and progressive inflammation of bones and joints [26–29].

Currently, colloidal gold is included in the category of food supplements and is used for antibacterial, antioxidant, and anti-age properties [27,30]. Recent research reported that different gold species possess anticancer, antiproliferative, antimicrobial, anti-inflammatory, antibacterial, anti-rheumatic, and antimalarial properties [27,29,31].

The latest research on the biomedical applications of gold nanoparticles (AuNPs) has shown potential in medical imaging, drug delivery systems, or therapeutic agents for cancer, HIV, neurodegenerative diseases (Alzheimer's, Parkinson's), nutrition diseases (diabetes, obesity), ophthalmology, and tissue engineering [28].

AuNPs display versatility, strong surface plasmon absorption, high stability, biocompatibility, and low toxicity in biological environments. Moreover, their high surface-to-volume ratio and predetermined size allow the functionalization of a wide variety of biologically active compounds. Hence, they are especially useful in the design of innovative materials, robust and selective for vectorization, imaging, diagnostics, and cancer therapy [28,31–33]. Hereafter, the design of a phyto-engineered-AuNPs carrier assembly will act as a selective vehicle with multi-targeted effects that exert a significant anti-proliferative effect [31–34].

There is relatively little research on Romanian viscum aimed mainly at determining certain constituents such as polyphenols, total proteins, amino acids, peptides, lectins, and viscotoxins from various parts of the plant (young leaves and branches). Moreover, most of these studies used viscum collected from *Acer campestre, Mallus domestica, Fraxinus excelsior, Populus nigra*, and *R. pseudoacacia* [5,35–40].

To our best knowledge, this study investigates for the first time the complete low-molecular-weight metabolite profile of the Romanian *Viscum album* hosted on *Quercus robur* L. (collected on summer solstice). Furthermore, our previous studies were focused on identifying the amino acids and thionines in viscum (collected near the winter solstice) from the same oak species [5].

The results of this study confirm, for the first time, the existence of a difference between the profile of amino acids and small peptides in the viscum samples grown on the same Romanian oak species and collected in the two periods considered critical by traditional European medicine.

Another novelty of this study is that, for the first time, an active, selective, and specific target-engineered carrier assembly with AuNPs features, which collectively capitalizes the therapeutic properties of Romanian viscum (whole plant), was developed and analyzed.

2. Results and Discussion

Plants, and medicinal plants in particular, contain a remarkable complex mixture of natural compounds with unique chemical structures and a significant number of stereogenic centers. A herb's biological activity is due to the synergistic interaction of all its compounds within an organism. Therefore, the pharmacological action of a plant extract is attributed to a whole multi-component mixture of constituent natural compounds [41–43].

On the other hand, an important aspect that must be considered for herb chemical screening, is that its metabolites profile varies depending on various endogenous or ecological factors [38,44,45].

Numerous research studies have focused on the highly complex phytochemical content of viscum. However, the correlation between their metabolic profiles and bioactivity has not yet been established. One of the main reasons is the variation in the composition of the phytoconstituents depending on the host tree [39,46,47].

A qualitative untargeted metabolomics profiling strategy based on a mass spectrometry approach is a powerful tool for fast and cost-effective chemical screening of secondary metabolites from natural compounds.

The chemical screening profile of low-molecular-weight metabolites from viscum was tentatively identified through electrospray ionization–quadrupole time-of-flight mass spectrometry (ESI-QTOF-MS) analysis. The mass spectra of the components identified were accomplished by connecting with those of NIST/EPA/NIH, Mass Spectral Library 2.0 database and reviewing the literature [46–51]. The mass spectrum and the components identified by ESI-QTOF-MS analysis are presented in Figure 1 and Table 1.

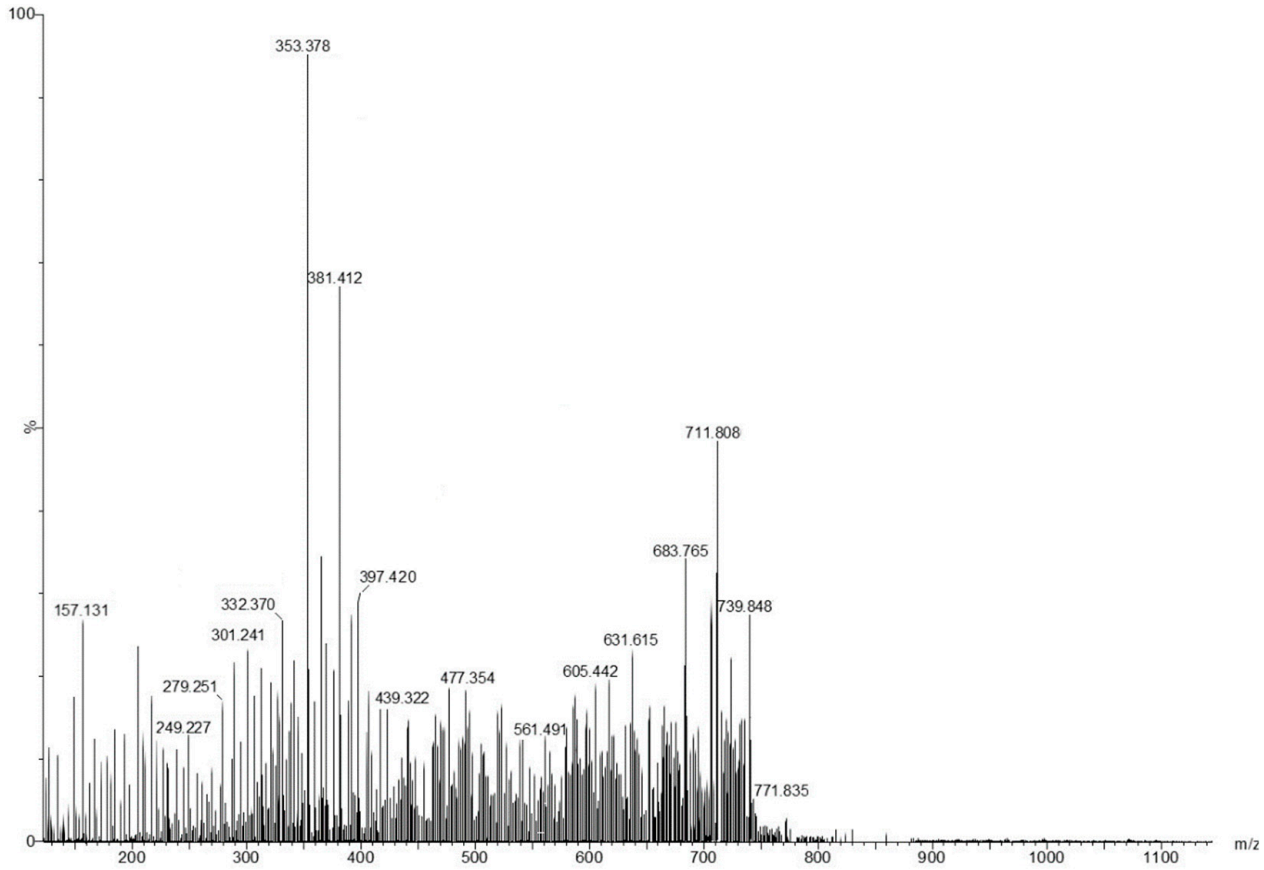

Figure 1. The mass spectrum of Romanian *Viscum album* hosted on *Quercus robur* L. (collected on summer solstice).

Table 1. Components identified through electrospray ionization–quadrupole time-of-flight mass spectrometry (ESI-QTOF-MS) analysis.

Compound No.	m/z Detected	Theoretic m/z	Formula	Tentative of Identification	Category	Ref.
1	104.16	104.17	$C_5H_{14}NO^+$	choline	amine	[48]
2	111.15	111.15	$C_5H_9N_3$	histamine	amine	[48]
3	121.14	121.16	$C_3H_7NO_2S$	cysteine	amino acids	[9]
4	122.15	122.16	$C_8H_{10}O$	2-phenylethanol	alcohol	[50]
5	128.22	128.21	$C_8H_{16}O$	1-octene-3-ol	alcohol	[51]
6	131.16	131.17	$C_6H_{13}NO_2$	leucine	amino acids	[52]
7	136.22	136.23	$C_{10}H_{16}$	sabinene	terpenoids	[51]
8	138.11	138.12	$C_7H_6O_3$	salicylic acid	phenolic acid	[10,40]
9	144.20	144.21	$C_8H_{16}O_2$	octanoic acid	fatty acids	[51]
10	146.13	146.14	$C_9H_6O_2$	coumarin	coumarins	[49]
11	146.22	146.21	$C_7H_{16}NO_2^+$	acetylcholine	amine	[48]
12	147.12	147.13	$C_5H_9NO_4$	glutamic acid	amino acids	[11,52]
13	148.15	148.16	$C_9H_8O_2$	cinamic acid	phenolic acid	[40]
14	149.22	149.21	$C_5H_{11}NO_2S$	methionine	amino acids	[52]
15	150.21	150.22	$C_{10}H_{14}O$	safranal	terpenoids	[51]
16	152.14	152.15	$C_8H_8O_3$	vanillin	aldehydes, phenols	[50]
17	152.21	152.23	$C_{10}H_{16}O$	citral	terpenoids	[51]
18	154.11	154.12	$C_7H_6O_4$	gentisic acid	phenolic acid	[10,40]
19	154.26	154.25	$C_{10}H_{18}O$	geraniol	terpenoids	[51]
20	155.14	155.15	$C_6H_9N_3O_2$	histidine	amino acids	[52]
21	156.21	156.22	$C_9H_{16}O_2$	nonanolide	lactone	[51]
22	162.17	162.18	$C_{10}H_{10}O_2$	cinnamic acid methyl ester	ester	[50]
23	164.14	164.16	$C_9H_8O_3$	p-coumaric acid	phenolic acid	[40,49]
24	166.18	166.17	$C_9H_{10}O_3$	tropic acid	organic acid	[52]
25	170.11	170.12	$C_7H_6O_5$	gallic acid	phenolic acid	[52]
26	174.10	174.11	$C_6H_6O_6$	aconic acid	miscellaneous	[52]
27	174.19	174.2	$C_6H_{14}N_4O_2$	arginine	amino acids	[11,48,52]
28	176.11	176.12	$C_6H_8O_6$	ascorbic acid	organic acid	[40,49]
29	176.16	176.17	$C_{10}H_8O_3$	6-hydroxy-4-methylcoumarin	coumarins	[52]
30	180.15	180.16	$C_9H_8O_4$	caffeic acid	phenolic acid	[40,52,53]
31	181.18	181.19	$C_9H_{11}NO_3$	tyrosine	amino acids	[11,52]
32	182.16	182.17	$C_9H_{10}O_4$	veratric acid	phenolic acid	[10]
34	186.11	186.12	$C_8H_{14}N_2O_3$	prolyl-alanine	dipeptide	[52]
35	188.21	188.22	$C_8H_{16}N_2O_3$	leucyl-glycine	dipeptide	[52]
36	192.11	192.12	$C_6H_8O_7$	citric acid	organic acid	[52]
37	193.16	192.17	$C_7H_{12}O_6$	quinic acid	organic acid	[49,53,54]
38	192.29	192.3	$C_{13}H_{20}O$	ionone	ketone	[51]
39	194.17	194.18	$C_{10}H_{10}O_4$	ferulic acid	phenolic acid	[10,40]
40	194.30	194.31	$C_{13}H_{22}O$	geranylacetone	terpenoids	[51]
41	196.23	196.24	$C_{11}H_{16}O_3$	loliolide	terpenoid	[52]
42	196.27	196.29	$C_{12}H_{20}O_2$	nerol acetate	terpenoids	[51]
43	198.16	198.17	$C_9H_{10}O_5$	syringic acid	phenolic acid	[40,53]
44	202.23	202.25	$C_9H_{18}N_2O_3$	leucyl-alanine	dipeptide	[52]

Table 1. *Cont.*

Compound No.	m/z Detected	Theoretic m/z	Formula	Tentative of Identification	Category	Ref.
45	204.21	204.22	$C_{11}H_{12}N_2O_2$	tryptophan	amino acids	[52]
46	204.34	204.35	$C_{15}H_{24}$	caryophyllene	terpenoids	[51]
47	204.36	206.37	$C_{15}H_{26}$	cadinene	terpenoids	[51,52]
48	208.19	208.21	$C_8H_{16}O_6$	viscumitol	saccharides	[49]
49	216.27	216.28	$C_{10}H_{20}N_2O_3$	valylvaline	dipeptide	[52]
50	222.35	222.37	$C_{15}H_{26}O$	cadinol	terpenoids	[51,52]
51	224.19	224.21	$C_{11}H_{12}O_5$	sinapic acid	phenolic acid	[40,53]
52	224.29	224.3	$C_{13}H_{20}O_3$	vomifoliol	terpenoids	[52]
53	226.21	226.23	$C_{11}H_{14}O_5$	genipin	terpenoids	[52]
54	228.28	228.29	$C_{11}H_{20}N_2O_3$	prolyl-leucine	dipeptide	[52]
55	229.22	229.23	$C_9H_{15}N_3O_4$	asparaginyl-proline	dipeptide	[52]
56	230.29	230.3	$C_{15}H_{18}O_2$	dehydrocostuslactone	terpenoids	[52]
57	234.19	234.2	$C_{12}H_{10}O_5$	7-methoxycoumarin-4-acetic acid	coumarins	[52]
58	234.37	234.38	$C_{15}H_{26}N_2$	sparteine	alkaloid	[55]
59	236.26	236.27	$C_{12}H_{16}N_2O_3$	phenylalanylalanine	dipeptide	[52]
60	236.34	236.35	$C_{15}H_{24}O_2$	curcumol	terpenoids	[52]
61	240.49	240.5	$C_{17}H_{36}$	heptadecane	hydrocarbons, lipids	[51]
62	242.21	242.23	$C_{10}H_{14}N_2O_5$	thymidine	nucleoside	[40,49]
63	242.39	242.4	$C_{15}H_{30}O_2$	pentadecanoic acid	fatty acids	[51]
64	243.21	243.22	$C_9H_{13}N_3O_5$	cytidine	nucleoside	[52]
65	244.19	244.2	$C_9H_{12}N_2O_6$	uridine	nucleoside	[52]
66	244.23	244.24	$C_{10}H_{16}N_2O_5$	prolylglutamic acid	dipeptide	[52]
67	244.31	244.33	$C_{12}H_{24}N_2O_3$	isoleucyl-isoleucine	dipeptide	[11,52]
68	248.35	248.36	$C_{15}H_{24}N_2O$	lupanine	alkaloid	[55]
69	250.26	250.27	$C_8H_{14}N_2O_5S$	gamma-glutamylcysteine	dipeptide	[49]
70	250.37	250.38	$C_{15}H_{26}N_2O$	retamine	alkaloid	[53]
71	256.41	256.42	$C_{16}H_{32}O_2$	palmitic acid	fatty acids	[52]
72	262.29	262.3	$C_{14}H_{18}N_2O_3$	prolylphenylalanine	dipeptide	[52]
74	264.31	264.32	$C_{14}H_{20}N_2O_3$	phenylalanylvaline	dipeptide	[52]
74	267.23	267.24	$C_{10}H_{13}N_5O_4$	adenosine	nucleoside	[40,52]
75	272.24	272.25	$C_{15}H_{12}O_5$	naringenin	flavonoids	[40,54,55]
76	278.29	278.3	$C_{14}H_{18}N_2O_4$	tyrosyl-L-proline	dipeptide	[55]
77	278.39	278.4	$C_{18}H_{30}O_2$	linolenic acid	fatty acids	[46]
78	278.33	278.35	$C_{15}H_{22}N_2O_3$	leucyl-phenylalanine	dipeptide	[52]
79	280.39	280.4	$C_{18}H_{32}O_2$	linoleic acid	fatty acids	[52]
80	283.21	283.24	$C_{10}H_{13}N_5O_5$	guanosine	nucleoside	[52]
81	284.49	284.5	$C_{18}H_{36}O_2$	stearic acid	fatty acids	[52]
82	286.23	286.24	$C_{15}H_{10}O_6$	luteolin	flavonoids	[52]
83	288.26	288.25	$C_{15}H_{12}O_6$	eriodictyol	flavonoids	[49]
84	292.39	292.4	$C_{18}H_{28}O_3$	9-OxoOTrE	fatty acids	[52]
85	292.34	294.35	$C_{15}H_{22}N_2O_4$	tyrosylleucine	dipeptide	[52]
86	296.49	296.5	$C_{20}H_{40}O$	phytol	terpenoids	[51]
87	298.39	298.4	$C_{19}H_{22}O_3$	acerogenin G	flavonoids	[46]
88	300.25	300.26	$C_{16}H_{12}O_6$	rhamnocitrin	flavonoids	[49]

Table 1. *Cont.*

Compound No.	m/z Detected	Theoretic m/z	Formula	Tentative of Identification	Category	Ref.
89	302.22	302.23	$C_{15}H_{10}O_7$	quercetin	flavonoids	[40,53,54]
90	302.27	302.28	$C_{16}H_{14}O_6$	homoeriodictyol	flavonoids	[46]
91	300.39	300.4	$C_{19}H_{24}O_3$	centrolobol	flavonoids	[46]
92	307.31	307.33	$C_{10}H_{17}N_3O_6S$	glutathione	peptides	[48,49,52]
93	308.49	308.5	$C_{20}H_{36}O_2$	terpineol	terpenoids	[51]
94	312.39	312.4	$C_{18}H_{20}N_2O_3$	phenylalanylphenylalanine	dipeptide	[52]
95	312.49	312.5	$C_{20}H_{40}O_2$	arachidic acid	fatty acids	[52]
96	314.27	314.29	$C_{17}H_{14}O_6$	ermanin	flavonoids	[52]
97	314.49	314.5	$C_{18}H_{34}O_4$	12,13-DiHOME	fatty acids	[52]
98	316.25	316.26	$C_{16}H_{12}O_7$	rhamnetin	flavonoids	[52]
99	317.39	317.4	$C_{17}H_{23}N_3O_3$	leucyl-tryptophan	dipeptide	[52]
100	328.39	328.4	$C_{19}H_{20}O_5$	hirsutanone	diarylheptanoids	[49,52]
101	330.27	330.29	$C_{17}H_{14}O_7$	rhamnazin	flavonoids	[49]
102	341.39	341.4	$C_{17}H_{31}N_3O_4$	Ile-Pro-Ile	peptides	[52]
103	342.33	342.34	$C_{16}H_{22}O_8$	coniferin	glucoside	[56]
104	344.39	344.3	$C_{18}H_{16}O_7$	santin	flavonoids	[52]
105	354.29	354.31	$C_{16}H_{18}O_9$	chlorogenic acid	phenolic acid	[40,46,49,54]
106	360.29	360.3	$C_{18}H_{16}O_8$	rosmarinic acid	phenolic acid	[10,40]
107	368.59	368.6	$C_{24}H_{48}O_2$	lignoceric acid	fatty acids	[52]
108	372.39	372.4	$C_{17}H_{24}O_9$	syringin	flavonoids	[11,52]
109	386.39	386.4	$C_{19}H_{30}O_8$	roseoside	terpenoids	[52]
110	388.39	388.4	$C_{21}H_{24}O_7$	medioresinol	lignal	[52]
111	399.69	399.7	$C_{26}H_{52}O_2$	cerotic acid	fatty acids	[52]
112	406.39	406.4	$C_{20}H_{22}O_9$	viscutin-3	flavonoids	[49]
113	412.69	412.7	$C_{30}H_{52}$	lupane	terpenoids	[49]
114	414.69	414.7	$C_{29}H_{50}O$	β-sitosterol	sterols	[49,57]
115	418.39	418.4	$C_{22}H_{26}O_8$	syringaresinol	lignal	[49]
116	426.69	426.7	$C_{30}H_{50}O$	lupeol	terpenoids	[46,49]
117	434.29	434.3	$C_{20}H_{18}O_{11}$	avicularin	flavonoids	[55]
118	434.39	434.4	$C_{21}H_{22}O_{10}$	naringenin-7-O-glucoside	flavonoids	[54]
119	442.39	442.4	$C_{20}H_{26}O_{11}$	visartiside D	flavonoids	[54]
120	442.69	442.7	$C_{30}H_{50}O_2$	betulin	terpenoids	[46]
121	448.39	448.4	$C_{21}H_{20}O_{11}$	quercitrin	flavonoids	[49]
122	450.39	450.4	$C_{21}H_{22}O_{11}$	eriodictyol-7-O-glucoside	flavonoids	[50]
123	456.69	456.7	$C_{30}H_{48}O_3$	betulinic acid	terpenoids	[46,57]
124	464.39	464.4	$C_{21}H_{20}O_{12}$	hyperoside	flavonoids	[51]
125	468.79	468.8	$C_{32}H_{52}O_2$	β-amyrin acetate	terpenoids	[50]
126	476.41	476.43	$C_{23}H_{24}O_{11}$	flavoyadorinin B	flavonoids	[49]
127	478.39	478.4	$C_{22}H_{22}O_{12}$	isorhamnetin-3-O-rutinoside	flavonoids	[52,53,56]
128	492.39	492.4	$C_{23}H_{24}O_{12}$	flavoyadorinin A	flavonoids	[49]
129	526.49	526.5	$C_{27}H_{26}O_{11}$	viscutin-1	flavonoids	[49]
130	532.49	532.5	$C_{27}H_{32}O_{11}$	visartiside E	flavonoids	[50]
131	536.89	536.9	$C_{40}H_{56}$	carotene	miscellaneous	[48]
132	565.79	565.8	$C_{30}H_{55}N_5O_5$	viscumamide	peptides	[58,59]

Table 1. *Cont.*

Compound No.	m/z Detected	Theoretic m/z	Formula	Tentative of Identification	Category	Ref.
133	568.49	568.5	$C_{29}H_{28}O_{12}$	viscutin-2	flavonoids	[49]
134	576.79	576.8	$C_{35}H_{60}O_6$	daucosterol	sterols	[52]
135	596.49	596.5	$C_{27}H_{32}O_{15}$	viscumneosides I	flavonoids	[49]
136	608.49	608.5	$C_{28}H_{32}O_{15}$	homoflavoyadorinin B	flavonoids	[52]
137	636.59	636.6	$C_{29}H_{32}O_{16}$	viscumneoside IV	flavonoids	[49]
138	728.59	728.6	$C_{32}H_{40}O_{19}$	viscumneoside V	flavonoids	[49]
139	768.69	768.7	$C_{34}H_{40}O_{20}$	viscumneoside VII	flavonoids	[49]
140	784.96	784.97	$C_{41}H_{68}O_{14}$	astragaloside IV	terpenoid	[49]

2.1. Screening and Classification of the Differential Metabolites

A total of 140 compounds were found and identified by mass spectroscopy analysis, including primary metabolites (amino acids, peptides, organic acids, nucleosides, etc.) and secondary metabolites (terpenoids, flavonoids, sterols, coumarins, alkaloids, phenolic acids, sterols, fatty acids, and miscellaneous), confirming the results reported in other studies on this plant [10,11,40–59]. These phytochemicals were assigned to different chemical categories: flavonoids (22.14%), amino acids and peptides (20%), terpenoids (17.85%), phenolic acids (7.85%), fatty acids (7.85%), organic acids (4.28%), nucleosides (3.57%), alcohols and esters (3.57%), coumarins (2.14%), alkaloids (2.14%), amines (2.14%), lignals (2.14%), sterols (1.42%), aldehydes and ketones (1.42%), and other. Flavonoids, amino acids and peptides, and terpenoids represent about 60% of all metabolites identified in *Viscum album*. The distribution of the identified metabolites in various chemical classes is listed in Table 2.

Table 2. Classification of metabolites from the *Viscum album* sample on different chemical categories.

Chemical Class	Metabolite Name
Flavonoids	naringenin
	acerogenin G
	luteolin
	eriodictyol
	rhamnocitrin
	centrolobol
	quercetin
	homoeriodictyol
	ermanin
	rhamnetin
	rhamnazin
	santin
	syringin
	viscutin-3
	avicularin
	naringenin-7-O-glucoside
	visartiside D
	quercitrin

Table 2. *Cont.*

Chemical Class	Metabolite Name
Flavonoids	eriodictyol-7-O-glucoside
	hyperoside
	flavoyadorinin B
	isorhamnetin-3-O-rutinoside
	flavoyadorinin A
	viscutin-1
	visartiside E
	viscutin-2
	viscumneosides I
	homoflavoyadorinin B
	viscumneoside IV
	viscumneoside V
Amino acids and peptides	cysteine
	leucine
	glutamic acid
	methionine
	histidine
	arginine
	tyrosine
	prolyl-alanine
	leucyl-glycine
	leucyl-alanine
	tryptophan
	valylvaline
	prolyl-leucine
	asparaginyl-proline
	phenylalanylalanine
	prolylglutamic acid
	isoleucyl-isoleucine
	gamma-glutamylcysteine
	prolylphenylalanine
	phenylalanylvaline
	tyrosyl-L-proline
	leucyl-phenylalanine
	tyrosylleucine
	glutathione
	phenylalanylphenylalanine
	leucyl-tryptophan
	Ile-Pro-Ile
	viscumamide

Table 2. *Cont.*

Chemical Class	Metabolite Name
Terpenoids	sabinene
	safranal
	citral
	geraniol
	geranylacetone
	loliolide
	nerol acetate
	caryophyllene
	cadinene
	cadinol
	vomifoliol
	genipin
	dehydrocostuslactone
	curcumol
	phytol
	acerogenin G
	terpineol
	hirsutanone
	roseoside
	lupane
	lupeol
	betulin
	betulinic acid
	β-amyrin acetate
	astragaloside IV
Phenolic acids	salicilyc acid
	cinamic acid
	gentisic acid
	p-coumaric acid
	gallic acid
	caffeic acid
	veratric acid
	ferulic acid
	syringic acid
	chlorogenic acid
	rosmarinic acid
Fatty acids	octanoic acid
	pentadecanoic acid
	palmitic acid
	linolenic acid

Table 2. *Cont.*

Chemical Class	Metabolite Name
Fatty acids	linoleic acid
	stearic acid
	9-OxoOTrE
	arachidic acid
	12,13-DiHOME
	lignoceric acid
	cerotic acid
Organic acids	tropic acid
	aconic acid
	ascorbic acid
	citric acid
	quinic acid
Nucleosides	thymidine
	cytidine
	uridine
	adenosine
	guanosine
Alcohols and esters	2-phenylethanol
	1-octene-3-ol
	cinnamic acid methyl ester
	viscumitol
	sinapic acid
Amines	choline
	histamine
	acetylcholine
Coumarins	coumarin
	6-hydroxy-4-methylcoumarin
	7-methoxycoumarin-4-acetic acid
Alkaloids	sparteine
	lupanine
	retamine
Lignals	pinoresinol
	medioresinol
	syringaresinol
Sterols	β-sitosterol
	daucosterol
Aldehydes and ketones	vanillin
	ionone

Table 2. *Cont.*

Chemical Class	Metabolite Name
Miscellaneous	nonanolide
	heptadecane
	carotene
	coniferin

Figure 2 presents the metabolite classification chart and was obtained on the basis of the data analysis reported in Table 2.

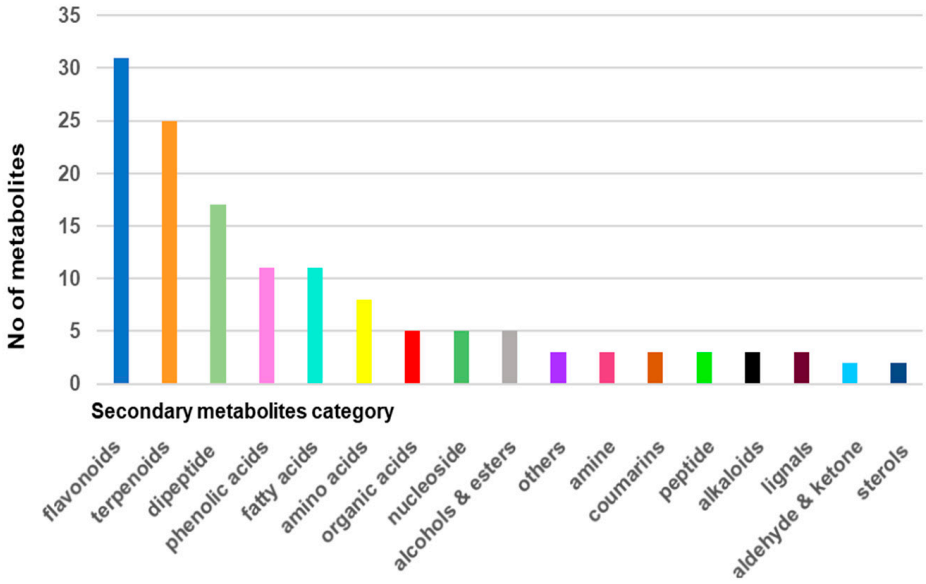

Figure 2. Metabolite classification bar chart of Romanian *Viscum album* hosted on *Quercus robur* L. (collected on summer solstice).

Amino acids and peptides: a total of 28 compounds were identified in the plant extract. A large part of these compounds (over 80%) is essential amino acids (phenylalanine, leucine, tryptophan, valine, methionine, histidine, and arginine). The non-essential amino acids (tyrosine, glutamic acid, cysteine, proline, glycine, alanine, and asparagine) are present only in a smaller proportion, about 20% of them [60–64]. The majority of the amino acids identified in the viscum sample (arginine, phenylalanine, tryptophan, histidine, glutamic acid, methionine, glycine, and proline) exhibit cytotoxicity, antiproliferative, and immunomodulant activity [61–65].

Several new small peptides (17 dipeptides, a cyclic peptide, and one tripeptide) have been identified, indicating that the profile of small peptides varies in the chemical composition of the viscum grown on the same oak species during the summer solstice and winter solstice [5]. This difference in the composition of small peptides in the viscum samples (on oak in the same geographical region) confirms the variation in plant therapeutic properties (especially antitumor and immunomodulatory) depending on the two periods considered essential in traditional European medicine [7,17].

Terpenoids and sesquiterpenes are among the main categories of metabolites found in viscum samples. Extensive studies report their antimicrobial, antioxidant, anticonvulsive, analgesic, neuroprotective, anti-inflammatory, anti-allergic, and antitumoral activities [51,60,65–68].

Coumarins are another class of phytoconstituents with high biological activity: antiviral, antimicrobial, antioxidant, analgesic, anticancer, anti-inflammatory, and anti-neurodegenerative [60,69]. Studies have shown coumarins' therapeutic applications in several types of cancer: leukemia, breast, renal, prostate, and malignant melanoma [65,70].

Flavonoids are the largest class of metabolites (over 30 different compounds) in the viscum sample. These biomolecules have numerous therapeutic effects: antioxidant, antitumoral, cardiovascular system protection (atherosclerosis, antiplatelet), antimicrobial, anti-inflammatory, and neurodegenerative diseases (Alzheimer) [60,65,71–73].

Phenolic acids are reported to act as an antioxidant, anti-inflammatory, antitumoral, neuroprotective, antimicrobial, and antidiabetic agents [60,65,74,75].

Sterol and steroids have been demonstrated to have anti-inflammatory, antitumoral, antidiabetic, antioxidant, anti-atherosclerotic, neuroprotective, immunomodulatory, osteoporosis protection, and cardiovascular protective (anti-atherosclerosis, anti-hemolytic) activities [60,65,76].

Fatty acids represent another important class of secondary metabolites, representing approximately 8% of the total metabolites identified in the viscum sample. Various studies highlight their importance for human health, such as anti-inflammatory, antioxidant, neuroprotective (stroke, Alzheimer's disease), and cardiovascular protective activity (anti-arrhythmic, dyslipidemia, hypertension, and anti-thrombotic) [60,65,77].

Carbohydrates and polysaccharides are biomolecules involved in the different beneficial roles for human health: anti-inflammatory, antiviral (anti-HIV), antioxidant (anti-ageing), digestive protection, cardio-protective, anti-arthritic, antibacterial, immunomodulatory, anti-diabetic, and anti-tumoral [60,65,78,79].

Glycosides are plant metabolites that act as antitumoral agents, especially for gastric cancer and chronic granulocytic leukemia [65,79].

Miscellaneous compounds, for instance, nonalide (lactone), identified in the viscum sample extract have antifungal activity, antimalarial, and cytotoxic activities [51].

2.2. Engineered Viscum–AuNPs Carrier Assembly

Development of targeted assembly rides on a robust and complex carrier assembly design that collectively combines the therapeutic properties of both components (viscum and an inorganic component) and the physicochemical characteristics of AuNPs (surface plasmon resonance, high surface area, conductivity, and low toxicity) [80–82].

Active targeting of an engineered carrier assembly relies upon a tailored surface to ensure high selectivity, vectorization, and specificity, and thus exert a significant therapeutic effect [80–85].

Development of targeted assembly rides on the construction of a robust, complex carried assembly that combines collectively the structural features of AuNPs (nontoxic, high biocompatibility and solubility, non-immunogenicity, and distinctive optical properties) with remarkable antitumor effects of both components (viscum and inorganic component) [28,34,80].

2.3. FT-IR Spectroscopy

The preparation of an engineered viscum–AuNPs carrier assembly was investigated by FT-IR spectroscopy to identify the functional groups specific to functional groups specific its two components, viscum and AuNPs. The individual FT-IR spectrum of the viscum and carrier assembly is shown in Figure 3a,b. The FT-IR absorption bands identified in the viscum sample are presented in Table 3.

The FTIR peak of AuNPs coated with trisodium citrate (surfactant) (Figure 3b) presents the vibrational bands characteristic of a surfactant: at 3460 cm^{-1} (associated with a H–OH stretching vibration) and 2918 cm^{-1}; at 2856 cm^{-1} (attributed with CH- asymmetric and symmetric stretching vibrations); at 1598 cm^{-1} (associated with a COO- stretching vibration); at 1395 cm^{-1}; and at 757 cm^{-1} (assigned to C–H bending).

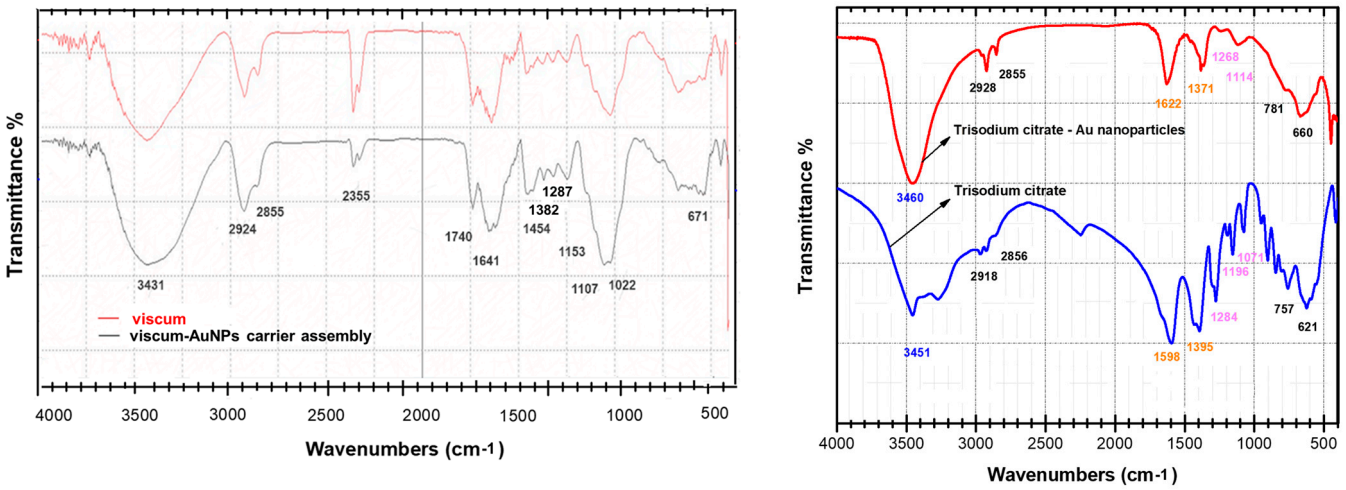

Figure 3. (**a**) FT-IR spectrum of the viscum sample and viscum–AuNPs carrier assembly; (**b**) FT-IR spectrum of AuNPs coated with trisodium citrate and the trisodium citrate spectrum.

Table 3. The characteristic group frequencies attributed to different metabolites identified in *Viscum album*.

Metabolites	Wavenumber (cm^{-1})	Ref.
Amino acids, peptides, thionins	3400; 3330–3130; 2530–2760; 2080–2140; 1724–1754 1687, 1675, 1663, 1654, 1644, 1632, 1621, 1611, 1610–1660, 1500–1600;	[5]
Flavonoids	1734, 1703, 1634, 1627, 1580, 1522, 1460, 1440, 1410, 1367, 1315, 1255, 630 and 575	[86–88]
Terpenoids	2938.7, 1740, 1651, 810	[87,89]
Phenolic acids	1800–1650, 1734, 1720, 1627, 1522, 1440, 1410, 1420–1300, 1367, 1315, 1255, 1170–1100	[88]
Fatty acids	3020–3010, 2924–2915, 2855–2847, 2800–2900, 1746, 1710, 1250, 720	[90,91]
Organic acids	1255, 1378, 1440, 1410, 1376	[88]
Nucleosides	968, 1120, 1175, 1330, 1420, 1480, 1725, 3270, 3600	[92]
Coumarins	600–900, 1200–1000, 1028, 1254, 1450, 1608, 1627–1715, 1740, 1760, 2207–2210, 2963, 3362, 3381, 3399, 3434,	[93,94]
Alkaloids	630–650, 925, 1200,1285, 1330, 1531, 1548, 1600–1650, 1653, 1658–1567, 1600, 1660, 1700, 1710, 3000, 3377, 3380, 3332, 3384.84	[95]
Sterols	740.5, 1062.5, 1192, 1383, 1465.6. 1737.5, 2937	[96]

The formation of an engineered viscum–AuNPs carrier assembly was successfully achieved and was confirmed through FT-IR spectroscopy. The spectra of nanoparticle carrier assembly (Figure 3a) show the characteristic absorption bands of the viscum sample as well as the AuNPs coated with a surfactant (trisodium citrate) (Figure 3a,b). In addition, the peaks at 1622, 1371, 1258, 1114, and 660 cm^{-1} were found in the synthesized AuNP solution (Figure 3a) and are shifted to higher wavenumbers (1641, 1382, 1267, 1153 and 671 cm^{-1}), indicating binding of nanoparticles to the functional groups O–H, C=O, C–N, C–S, and C–O belonging to the various phytoconstituents (Figure 3a,b and Table 3) [79–91]. In particular, the hydroxyl group is considered to be involved in the binding of AuNPs [85–98].

2.4. X-ray Diffraction Spectroscopy

Figure 4a,b present the XRD patterns of the AuNPs, viscum sample, and the engineered viscum–gold nanoparticles carrier assembly.

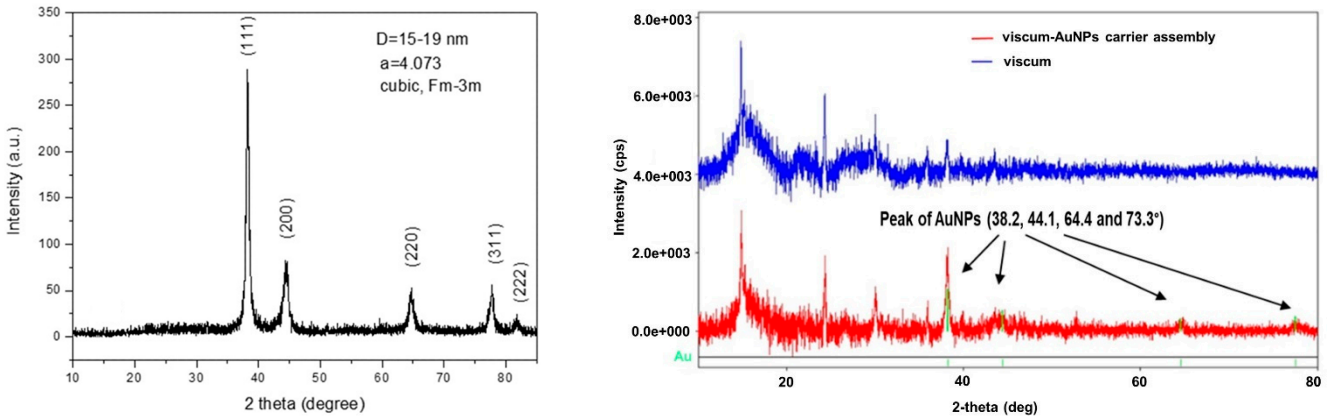

(**a**) (**b**)

Figure 4. (**a**) Powder XRD patterns of the AuNPs; (**b**) XRD patterns of the viscum sample and engineered viscum–AuNPs carrier assembly.

Figure 4a shows the specific XRD spectrum of AuNPs. The mean diameter (D) of the gold crystallites, calculated by using the Debye–Scherrer formula, was less than 20 nm. The AuNPs were well crystalized, with well-defined peaks.

The diffraction pattern of the viscum (Figure 4b) is in the range of 12–45°, with large bands and weak peaks characteristic of amorphous phases that can be attributed to plant fibers and minerals in the form of hydroxide.

The pattern of the engineered viscum–AuNPs carrier assembly has a shape similar to that of the viscum. In this spectrum, besides the wide bands and the weak peaks of the plant, one can observe, but much attenuated, the peaks of the AuNPs at 38.2, 44.1, 64.4, and 77.3°.

2.5. Scanning Electron Microscopy (SEM)

The SEM images of the synthesized AuNP solution, viscum sample, and engineered herb–AuNPs carrier assembly are presented in Figures 5–9. SEM micrographs of the AuNPs (Figure 5a) indicate a surface structure with agglomerated regions of regular, spherical particles, with dimensions between 8 and 18 nm [99]. The morphology of the viscum sample (Figure 6a,b) displays a fibrous structure surface, with irregular, porous areas with dimensions less than 1 mm. The presence of pores suggests an easy fixation of AuNPs on the surface of the plant sample.

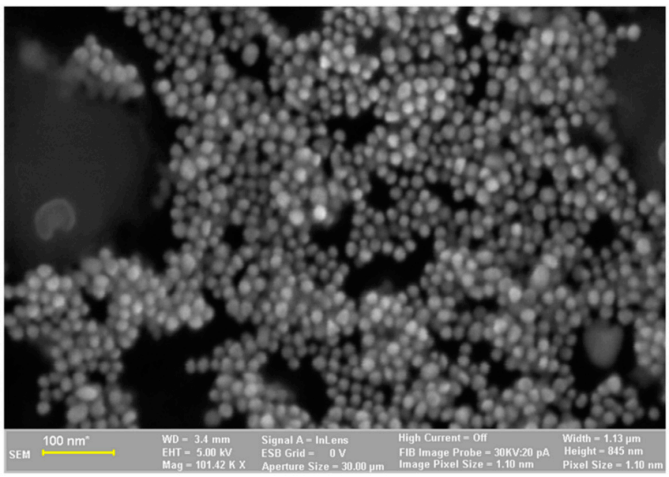

Figure 5. Two-dimensional image of the AuNPs obtained by the SEM technique.

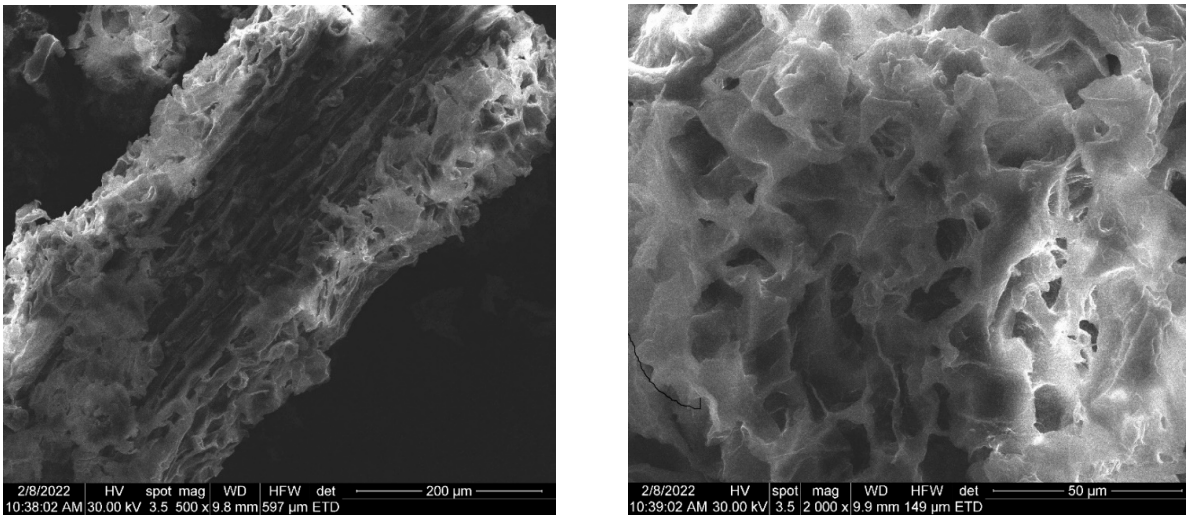

(**a**) (**b**)

Figure 6. (**a**) Two-dimensional image of the viscum sample obtained by the SEM technique (magnitude 200 µm). (**b**) Two-dimensional image of the viscum sample obtained by the SEM technique (magnitude 50 µm).

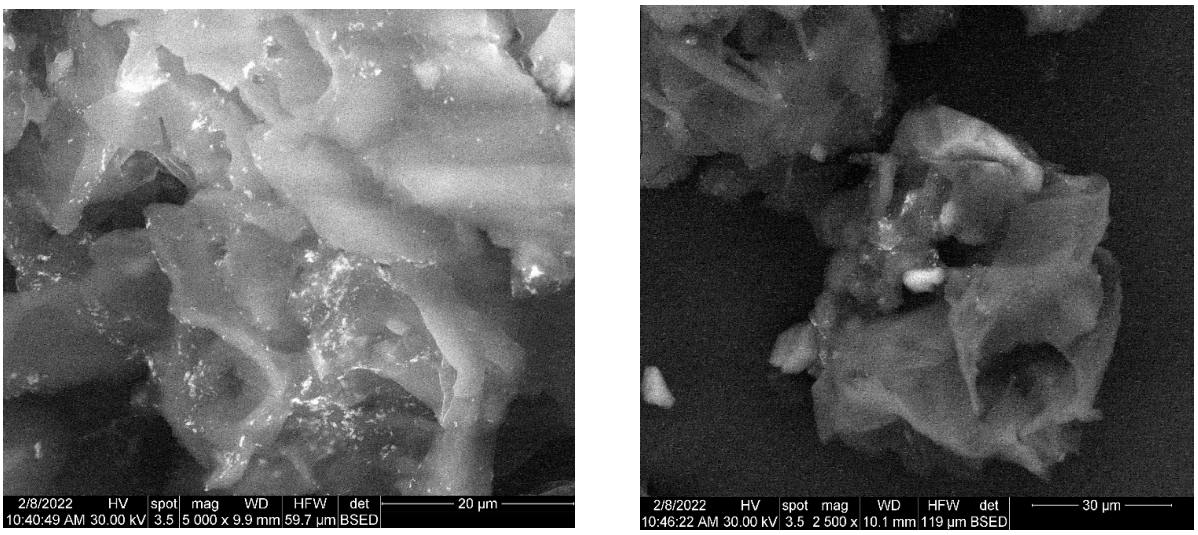

(**a**) (**b**)

Figure 7. (**a**) Two-dimensional image of the engineered viscum–AuNPs carrier assembly obtained by the SEM technique (magnitude 20 µm). (**b**) Two-dimensional image of the engineered viscum–AuNPs carrier assembly obtained by the SEM technique (magnitude 30 µm).

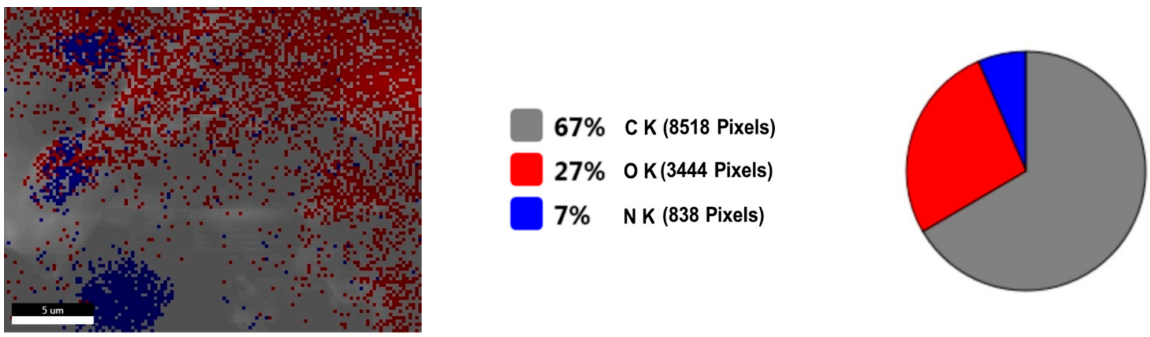

Figure 8. *Viscum* sample: SEM—live map.

Figure 9. Engineered viscum–AuNPs carrier assembly: SEM—live map.

The morphology of engineered viscum–AuNPs carrier assembly indicates the presence of AuNPs and agglomerations of AuNPs, fixed on the surface of viscum particles (Figure 7a) as well as loaded into the pores of viscum particles (Figure 7b).

Figure 8 shows the live map of viscum and the distribution of the identified elements. Figure 9 shows the live map for the engineered viscum–AuNPs carrier assembly and the distribution of the identified elements. The comparative analysis of Figure 8 shows the live map for viscum and engineered viscum–AuNPs carrier assembly (Figure 9) and highlights the presence of differences regarding the proportion of identification elements in the two samples, due to the formation of the viscum–metal carrier assembly. SEM analysis and live map confirms the obtaining of the engineered viscum–AuNPs carrier assembly [74].

2.6. UV–VIS Spectroscopy

The optical properties (surface plasmon resonance) of AuNPs and the achievement of an engineered viscum–AuNPs carrier assembly were monitored through UV–Vis spectroscopy.

In Figure 10a, it can be seen that AuNPs show a peak absorption at 526 nm, but this absorption band is not visible in the case of the engineered viscum–AuNPs carrier assembly. The viscum absorption spectra and the final material (engineered viscum–AuNPs carrier assembly) do not show significant differences. Moreover, the specific absorption peak of the AuNPs is not visible in the spectrum of viscum–AuNPs. However, there is a clear difference in the absorbance intensity between the first two spectra, starting at about 475 nm. This was better emphasized by subtracting the viscum spectrum from the spectrum of the engineered viscum–AuNPs carrier assembly (Figure 10b). After subtraction, the surface plasmon band (at 526 nm) in the spectrum of AuNPs is now discreetly observed also in the subtraction curve, even if the profiles of the curves match approximately up to 526 nm only. This demonstrates that viscum successfully incorporated the AuNPs and that the engineered viscum–AuNPs carrier assembly was obtained.

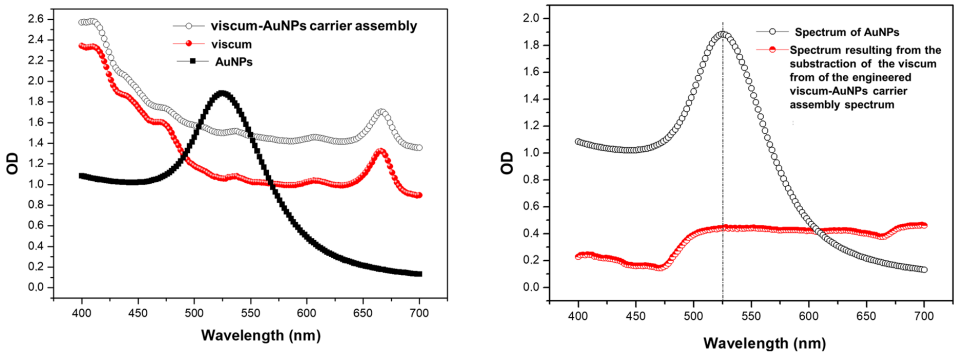

(**a**) (**b**)

Figure 10. (**a**) UV–Vis spectra of the AuNPs, viscum, and engineered viscum–AuNPs carrier assembly respectively. (**b**) UV–Vis spectrum resulting from subtracting the UV–VIS spectra of the AuNPs from the UV–Vis spectrum of the engineered viscum–AuNPs carrier assembly.

3. Materials and Methods

All used reagents were analytical grade. Methanol and chloroform were purchased from VWR (Wien, Austria) and used without further purification.

3.1. Carrier Assembly Components Preparation

AuNPs Synthesis

The citrate synthesis of gold nanoparticles was achieved by the following procedure: in conical flasks (2000 mL), 0.5 g $AuCl_4H$ was weighted and a constant volume (1450 mL) of ultrapure water was added under magnetic stirring (800 rpm). Then, 50 mL of sodium citrate solution (1.6%) was added rapidly. The mixture was kept at room temperature (22 °C) for 40 min and 800 rpm.

3.2. Plant Sample Preparation

The five individual viscum (*Viscum album L*) samples (whole plant) were collected from three trees (*Quercus robur* L.) in June 2021 from the area of Timis county, Romania (geographic coordinates 45°47′5″ N 21°16′0″ E), and were taxonomically authenticated at West University of Timisoara, Romania. The plant samples were rapidly frozen in liquid nitrogen (190 °C), ground and sieved to obtain a particle size lower than 0.5 mm, and kept at −40 °C to avoid enzymatic conversion or metabolite degradation.

3.3. Plant Preparation for Chemical Screening

For each analysis, 1.5 g of dried viscum sample was subject to sonication extraction in 25 mL of solvent (methanol/chloroform = 1:1) for 30 min at 38 °C with a frequency of 60 kHz. The solution was concentrated using a rotavapor and the residue was dissolved in MeOH. The extract was centrifuged, and the supernatant was filtered through a 0.2 µm syringe filter and stored at –18 °C until analysis until MS analysis. All samples were prepared in triplicate.

3.4. Mass Spectrometry

The experiments were conducted using EIS-QTOF-MS from Bruker Daltonics, Bremen, Germany. All mass spectra were acquired in the positive ion mode within a mass range of 100–3000 m/z, with a scan speed of 2.1 scans/s. The source block temperature was kept at 80 °C. The reference provided a spectrum in positive ion mode with fair ionic coverage of the m/z range scanned in full-scan MS. The resulting spectrum was a sum of scans over the total ion current (TIC) acquired at 25–85 eV collision energy to provide the full set of diagnostic fragment ions.

The metabolites were identified via comparison of their mass spectra with those of the standard library NIST/NBS-3 (National Institute of Standards and Technology/National Bureau of Standards) spectral database and the identified phytoconstituents are presented in Table 1.

3.5. Phyto-Engineered AuNPs Carrier Assembly Preparation

For each analysis, 2.5 g of sample was prepared from dried viscum (whole plant, ground and sieved to obtain a particle size lower than 0.5 mm) and a AuNPs solution was added (viscum/AuNPs nanoparticles = 1:4) at room temperature (22 °C) and under magnetic stirring (400 rpm) for 24 h. The obtained mixture was filtered (Φ185 mm filter paper) and then dried in oven at 40 °C for 4 h.

3.6. Characterisation of the Engineered Viscum–AuNPs Carrier Assembly

3.6.1. UV–Vis Analysis

The measurements were conducted using a spectrophotometer UV–VIS Perkin-Elmer Lambda 35 packing pre-aligned halogen and deuterium lamps. The two sources of radiation cover the range of wavelengths of 190–1100 nm and a variable bandwidth range of 0.5 to 4 nm.

3.6.2. Fourier Transform Infrared (FTIR) Spectroscopy

FTIR spectra were obtained by using the KBr pellet method ranging from 4000 cm^{-1} to 400 cm^{-1}, with a Perkin-Elmer Spectrum 100 FT-IR (Perkin–Elmer, Waltham, MA, USA).

The X-ray powder diffraction (XRD) pattern was performed using a Rigaku Ultima IV diffractometer equipped with a D/teX ultra-detector and operating at 40 kV and 40 mA, with monochromatic CuKα radiation (λ = 1.5406Å), in the 2θ range 10–80°, with a scan speed of 5°/min and a step size of 0.01°. The XRD patterns were compared with those from the ICDD Powder Diffraction Database, (ICDD file 04-015-9120). The average crystallite size and the phase content was calculated using the whole pattern profile fitting method (WPPF).

Scanning electron microscopy (SEM) micrographs were obtained with an SEM-EDS system (QUANTA INSPECT F50) equipped with a field-emission gun (FEG), 1.2 nm resolution, and energy dispersive X-ray spectrometer (EDS) with an MnK resolution of 133 eV.

4. Conclusions

In this study, the low molecular mass metabolites profiling of *Viscum album* (growing wild in Romania and hosted on *Quercus robur* L.) was accomplished. The biological activities were discussed for each metabolite category. Compared to our previous studies, 19 new small peptides were identified, which indicates that the profile of small peptides varies in the chemical composition of the viscum grown on the same oak species during the summer solstice and winter solstice.

Furthermore, a new and specific target-engineered viscum–AuNPs carrier assembly, with unique optical properties and great potential to increase the effectiveness of antitumor action and reduce unwanted side effects, was developed. The complete morpho-structural characterization of the viscum–AuNPs carrier assembly was performed. Further research is necessary to investigate the biological activity and biocompatibility of viscum extracts and the newly engineered viscum–AuNPs carrier assembly.

Author Contributions: Conception and design of study: A.-E.S. and I.G.; methodology: A.-E.S. and C.N.M.; acquisition of data: C.M. and C.N.M.; analysis and interpretation of data: C.N.M., C.M. and D.D.H.; writing—original draft preparation: I.S.; writing—review and editing: A.-E.S. and C.N.M.; investigation: I.S., C.M. and D.D.H. All authors have read and agreed to the published version of the manuscript.

Funding: This research received no external funding.

Institutional Review Board Statement: Not applicable.

Informed Consent Statement: Not applicable.

Data Availability Statement: Not applicable.

Acknowledgments: National Center for Micro and Nanomaterials (the center is part of the Department of Science and Engineering of Oxide and Nanomaterials Materials of the Faculty of Applied Chemistry and Materials Science of the Polytechnic University of Bucharest).

Conflicts of Interest: The authors declare no conflict of interest.

References

1. Barlow, B. Mistletoe in Folk Legend and Medicine. 2008. Available online: https://www.anbg.gov.au/mistletoe/folk-legend.html (accessed on 2 June 2022).
2. Frazer, J.G. *The Golden Bough: A Study in Magic and Religion*; Palgrave Macmillan: London, UK, 1990.
3. Gill, L.S.; Hawksworth, F.G. *The Mistletoes: A Literature Review*; U.S. Dept. Agr. Tech. Bul. 1242. U.S.; Government Printing Office: Washington, DC, USA, 1961. Available online: https://handle.nal.usda.gov/10113/CAT87201185 (accessed on 2 June 2022).
4. Ogunmefun, O.T.; Olatunji, B.P.; Adarabioyo, M.I. Ethnomedicinal Survey on the Uses of Mistletoe in South-Western Nigeria. *Eur. J. Med. Plants* **2015**, *8*, 224–230. [CrossRef]
5. Segneanu, A.; Velciov, S.M.; Olariu, S.; Cziple, F.; Damian, D.; Grozescu, I. Bioactive molecules profile from natural compounds. In *Amino Acid-New Insights and Roles in Plant and Animal*; Asao, T., Asaduzzaman, M., Eds.; IntechOpen: Rijeka, Croatia, 2017.

6. Szurpnicka, A.; Kowalczuk, A.; Szterk, A. Biological activity of mistletoe: In vitro and in vivo studies and mechanisms of action. *Arch. Pharm. Res.* **2020**, *43*, 593–629. [CrossRef]
7. Kleszken, E.; Timar, A.V.; Memete, A.R.; Miere (Groza), F.; Vicas, S.I. On overview of bioactive compounds, biological and pharmacological effects of mistletoe (*Viscum album* L.). *Pharmacophore* **2022**, *13*, 10–26. [CrossRef]
8. Freuding, M.; Keinki, C.; Micke, O.; Buentzel, J.; Huebner, J. Mistletoe in oncological treatment: A systematic review. *J. Cancer Res. Clin. Oncol.* **2019**, *145*, 695–707. [CrossRef] [PubMed]
9. Mazalovska, M.; Calvin Kouokam, J. Plant-derived lectins as potential cancer therapeutics and diagnostic tools. *BioMed Res. Int.* **2020**, *2020*, 1–13. [CrossRef]
10. Pietrzak, W.; Nowak, R. Impact of harvest conditions and host tree species on chemical composition and antioxidant activity of extracts from *Viscum album* L. *Molecules* **2021**, *26*, 3741. [CrossRef]
11. Jäger, T.; Holandino, C.; Melo, M.N.D.O.; Peñaloza, E.M.C.; Oliveira, A.P.; Garrett, R.; Glauser, G.; Grazi, M.; Ramm, H.; Urech, K.; et al. Metabolomics by UHPLC-Q-TOF Reveals Host Tree-Dependent Phytochemical Variation in *Viscum album* L. *Plants* **2021**, *10*, 1726. [CrossRef]
12. Majeed, M.; Rehman, R.U. Phytochemistry, Pharmacology, and Toxicity of an Epiphytic Medicinal Shrub *Viscum album* L. (White Berry Mistletoe). In *Medicinal and Aromatic Plants*; Aftab, T., Hakeem, K.R., Eds.; Springer: Cham, Switzerland, 2021; pp. 287–301.
13. Yuan, H.; Ma, Q.; Ye, L.; Piao, G. The traditional medicine and modern medicine from natural products. *Molecules* **2016**, *21*, 559. [CrossRef]
14. Loef, M.; Walach, H. Quality of life in cancer patients treated with mistletoe: A systematic review and meta-analysis. *BMC Complement Med. Ther.* **2020**, *20*, 227. [CrossRef]
15. Oei, S.L.; Thronicke, A.; Schad, F. Mistletoe and immunomodulation: Insights and implications for anticancer therapies. *Evid.-Based Complementary Altern. Med.* **2019**, *2019*, 1–6. [CrossRef]
16. Marvibaigi, M.; Supriyanto, E.; Amini, N.; Abdul Majid, F.A.; Jaganathan, S.K. Preclinical and clinical effects of mistletoe against breast cancer. *Biomed Res. Int.* **2014**, *2014*, 1–15. [CrossRef] [PubMed]
17. Urech, K.; Schaller, G.; Jäggy, C. Viscotoxins, mistletoe lectins and their isoforms in mistletoe (*Viscum album* L.) extracts Iscador. *Arzneimittelforschung* **2011**, *56*, 428–434. [CrossRef]
18. Vang Petersen, P. Warrior art, religion and symbolism. In *The Spoils of Victory. The North in the Shadow of the Roman Empire*; Jørgensen, L., Storgaard, B., Thomsen, L.G., Eds.; National Museet: Copenhagen, Denmark, 2003; pp. 286–293.
19. Available online: https://finds.org.uk/staffshoardsymposium/papers/charlottebehr (accessed on 2 June 2022).
20. Huaizhi, Z.; Yuantao, N. China's ancient gold drugs. *Gold Bull.* **2001**, *34*, 24–29. [CrossRef]
21. Patil-Bhole, T.; Wele, A.; Gudi, R.; Thakur, K.; Nadkarni, S.; Panmand, R.; Kale, B. Nanostructured gold in ancient Ayurvedic calcined drug 'swarnabhasma'. *J. Ayurveda Integr. Med.* **2021**, *12*, 640–648. [CrossRef]
22. Sharma, R.; Prajapati, P.K. Nanotechnology in medicine: Leads from Ayurveda. *J. Pharma Bioallied Sci. Jan.-Mar.* **2016**, *8*, 80–81. [CrossRef] [PubMed]
23. Parimalam, S.S.; Badilescu, S.; Bhat, R.; Packirisamy, M. A narrative review of scientific validation of gold- and silver-based Indian medicines and their future scope. *Longhua Chin. Med.* **2020**, *3*, 10. [CrossRef]
24. Metwaly, A.M.; Ghoneim, M.M.; Eissa, I.H.; Elsehemy, I.A.; Mostafa, A.E.; Hegazy, M.M.; Afifi, W.M.; Dou, D. Traditional ancient Egyptian medicine: A review. *Saudi J. Biol. Sci.* **2021**, *28*, 5823–5832. [CrossRef]
25. Forshaw, R.J. The practice of dentistry in ancient Egypt. *Br. Dent. J.* **2009**, *206*, 481–486. [CrossRef]
26. Console, R. Pharmaceutical use of gold from antiquity to the seventeenth century. *Geol. Soc. Lond. Spec. Publ.* **2013**, *375*, 171–191. [CrossRef]
27. Pricker, S.P. Medical uses of gold compounds: Past, present and future. *Gold Bull.* **1996**, *29*, 53–60. [CrossRef]
28. Balfourier, A.; Kolosnjaj-Tabi, J.; Luciani, N.; Carn, F.; Gazeau, F. Gold-based therapy: From past to present. *Proc. Natl. Acad. Sci. USA* **2020**, *117*, 22639–22648. [CrossRef] [PubMed]
29. Wang, H.H.; Su, C.H.; Wu, Y.J.; Lin, C.A.J.; Lee, C.H.; Shen, J.L.; Yeh, H.I. Application of gold in biomedicine: Past, present and future. *Int. J. Gerontol.* **2012**, *6*, 1–4. [CrossRef]
30. Medici, S.; Peana, M.F.; Zoroddu, M.A. Noble metals in pharmaceuticals: Applications and limitations. In *Biomedical Applications of Metals*; Rai, M., Ingle, A., Medici, S., Eds.; Springer: Cham, Switzerland, 2018; pp. 3–48.
31. Ott, I. On the medicinal chemistry of gold complexes as anticancer drugs. *Coord. Chem. Rev.* **2009**, *253*, 1670–1681. [CrossRef]
32. Goddard, Z.R.; Marín, M.J.; Russell, D.A.; Searcey, M. Active targeting of gold nanoparticles as cancer therapeutics. *Chem. Soc. Rev.* **2020**, *49*, 8774–8789. [CrossRef] [PubMed]
33. Yafout, M.; Ousaid, A.; Khayati, Y.; El Otmani, I.S. Gold nanoparticles as a drug delivery system for standard chemotherapeutics: A new lead for targeted pharmacological cancer treatments. *Sci. Afr.* **2021**, *11*, e00685. [CrossRef]
34. Yang, Z.; Wang, D.; Zhang, C.; Liu, H.; Hao, M.; Kan, S.; Liu, D.; Liu, W. The Applications of gold nanoparticles in the diagnosis and treatment of gastrointestinal cancer. *Front. Oncol.* **2022**, *11*, 819329. [CrossRef]
35. Vlad, D.C.; Popescu, R.; Dumitrascu, V.; Cimporescu, A.; Vlad, C.S.; Vágvölgyi, C.; Krisch, J.; Dehelean, C.; Horhat, F.G. Phytocomponents identification in mistletoe (*Viscum album*) young leaves and branches, by GC-MS and antiproliferative effect on HEPG2 And MCF7 cell lines. *Farmacia* **2016**, *64*, 82–87.
36. Paun, G.; Rotinberg, P.; Mihai, C.; Neagu, E.; Radu, G.L. Cytostatic activity of *Viscum album* L. extract processed by microfiltration and ultrafiltration. *Rom. Biotechnol. Lett.* **2011**, *16*, 6000–6007.

37. Vicas, S.I.; Socaciu, C. The biological activity of European mistletoe (*Viscum album*) extracts and their pharmaceutical impact. *Bull. USAMV-CN* **2007**, *63*, 217–222.
38. Sevastre, B.; Olah, N.K.; Hanganu, D.; Sárpataki, O.; Taulescu, M.; Mănălăchioae, R.; Marcus, I.; Cătoi, C. *Viscum album* L. alcoholic extract enhance the effect of doxorubicin in ehrlich carcinoma tumor cells. *Rom. Biotechnol. Lett.* **2012**, *17*, 6976–6981.
39. Stan, R.L.; Hangan, A.C.; Dican, L.; Sevastre, B.; Hanganu, D.; Catoi, C.; Sarpataki, O.; Ionescu, C.M. Comparative study concerning mistletoe viscotoxins antitumor activity. *Acta Biol. Hung.* **2013**, *64*, 279–288. [CrossRef] [PubMed]
40. Vicaş, S.I.; Rugina, D.; Leopold, L.; Pintea, A.; Socaciu, C. HPLC Fingerprint of bioactive compounds and antioxidant activities of *Viscum album* from different host trees. *Not. Bot Hort Agrobot Cluj* **2011**, *39*, 48–57. [CrossRef]
41. Yarnell, E. Synergy in Herbal Medicines: Part. *J. Restor. Med.* **2015**, *1*, 460–473. [CrossRef]
42. Zhao, Q.; Luan, X.; Zheng, M.; Tian, X.H.; Zhao, J.; Zhang, W.D.; Ma, B.L. Synergistic mechanisms of constituents in herbal extracts during intestinal absorption: Focus on natural occurring nanoparticles. *Pharmaceutics* **2020**, *12*, 128. [CrossRef]
43. Hussein, R.A.; El-Anssary, A.A. Plants secondary metabolites: The key drivers of the pharmacological actions of medicinal plants. In *Herbal Medicine*; Philip, F., Builders, Eds.; IntechOpen: Rijeka, Croatia, 2018.
44. Chen, G.; Wang, S.; Huang, X.; Hong, J.; Du, L.; Zhang, L.; Ye, L. Environmental factors affecting growth and development of Banlangen (*Radix Isatidis*) in China. *Afr. J. Plant. Sci.* **2015**, *9*, 421–426.
45. Pang, Z.; Chen, J.; Wang, T.; Gao, C.; Li, Z.; Guo, L.; Xu, J.; Cheng, Y. Linking plant secondary metabolites and plant microbiomes: A Review. *Front. Plant. Sci.* **2021**, *12*, 621276. [CrossRef]
46. Li, Y.; Zhao, Y.L.; Yang, Y.P.; Li, X.L. Chemical constituents of Viscum album var. meridianum. *Biochem. Syst. Ecol.* **2011**, *39*, 849–852. [CrossRef]
47. Singh, B.N.; Saha, C.; Galun, D.; Dalip, K.U.; Bayry, J.; Kaveri, S.V. European *Viscum album*: A potent phytotherapeutic agent with multifarious phytochemicals, pharmacological properties and clinical evidence. *RSC Adv. R. Soc. Chem.* **2016**, *6*, 23837–23857. [CrossRef]
48. Urech, K.; Baumgartner, S. *Chemical Constituents of Viscum Album L. Implications for the Pharmaceutical Preparation of Mistletoe in Mistletoe: From Mythology to Evidence-Based Medicine*; Zanker, K.S., Kaveri, S.V., Eds.; Transl Res Biomed; Karger: Basel, Switzerland, 2015; Volume 4, pp. 11–23.
49. Song, C.; Wei, X.-Y.; Qiu, Z.-D.; Gong, L.; Chen, Z.-Y.; Ma, Y.; Shen, Y.; Zhao, Y.-J.; Wang, W.-H.; Lai, C.-J.-S.; et al. Exploring the resources of the genus Viscum for potential therapeutic applications. *J. Ethnopharmacol.* **2021**, *277*, 114233. [CrossRef]
50. Patel, B.P.; Singh, P.K. *Viscum articulatum* Burm. F.: A review on its phytochemistry, pharmacology and traditional uses. *J. Pharm Pharm.* **2018**, *70*, 159–177. [CrossRef]
51. Wang, Q.; Chen, D.; Zhang, Q.; Qin, D.; Jiang, X.; Li, H.; Fang, l.; Cao, J.; Wu, H. Volatile components and nutritional qualities of *Viscum articulatum* Burm.f. parasitic on ancient tea trees. *Food Sci. Nutr.* **2019**, *7*, 3017–3029. [CrossRef] [PubMed]
52. Peñaloza, E.; Holandino, C.; Scherr, C.; de Araujo, P.I.P.; Borges, R.M.; Urech, K.; Baumgartner, S.; Garrett, R. Comprehensive metabolome analysis of fermented aqueous extracts of Viscum album L. by Liquid chromatography-high resolution tandem mass spectrometry. *Molecules* **2020**, *25*, 4006. [CrossRef] [PubMed]
53. Stefanucci, A.; Zengin, G.; Llorent-Martinez, E.J.; Dimmito, M.P.; Della Valle, A.; Pieretti, S.; Gunes, A.K.; Sinan, K.I.; Mollica, A. *Viscum album* L. homogenizer-assisted and ultrasound-assisted extracts as potential sources of bioactive compounds. *J. Food Biochem.* **2020**, *44*, e13377. [CrossRef] [PubMed]
54. Holandino, C.; Melo, M.N.; Oliveira, A.P.; da Costa Batista, J.V.; Capella, M.A.M.; Garrett, R.; Grazi, M.; Ramm, H.; Torre, C.D.; Schaller, G.; et al. Phytochemical analysis and in vitro anti-proliferative activity of *Viscum album* ethanolic extracts. *BMC Complement. Med.* **2020**, *20*, 215. [CrossRef]
55. Chandra, K. Bio Active Compounds Isolated from Mistletoe (*Scurulla Oortiana* (Korth) Danser Parasiting Tea Plant *Camellia sinenis* L.). Master's Thesis, University of Adelaide, Adelaide, Australia, 1996.
56. Fukunaga, T.; Kajikawa, I.; Nashiya, K.; Watanabe, Y.; Suzuki, N.; Takeya, K.; Itokawa, H. Studies on the constituents of the European mistletoe, *Viscum album* L.II. *Chem. Pharm. Bull.* **1988**, *36*, 1185–1189. [CrossRef]
57. Maher, S.; Fayyaz, S.; Naheed, N.; Dar, Z. The Isolation and screening of the bioactive compound of *Viscum album* against *Meloidogyne incognita*. *Pak. J. Nematol.* **2021**, *39*, 46–51. [CrossRef]
58. Oluwaseun, A.A.; Ganiyu, O. Antioxidant properties of methanolic extracts of mistletoes (*Viscum album*) from cocoa and cashew trees in Nigeria. *Afr. J. Biotechnol.* **2008**, *7*, 3138–3142.
59. Park, B.J.; Matsuta, T.; Samejima, H.; Park, C.H. In Chemical constituents of mistletoe (*Viscum album* L. var. coloratum Ohwi) Sung, J.; Lee, B.D.; Onjo, M. *IOSR J. Pharm. Biol. Sci.* **2017**, *12*, 19–23.
60. Das, K.; Gezici, S. Secondary plant metabolites, their separation and identification, and role in human disease prevention. *Ann. Phytomedicine Int. J.* **2018**, *7*, 13–24. [CrossRef]
61. Kim, S.-H.; Roszik, J.; Grimm, E.A.; Ekmekcioglu, S. Impact of *L*-arginine metabolism on immune response and anticancer immunotherapy. *Front. Oncol.* **2018**, *8*, 67. [CrossRef]
62. Chiangjong, W.; Chutipongtanate, S.; Hongeng, S. Anticancer peptide: Physicochemical property, functional aspect and trend in clinical application (Review). *Int. J. Oncol.* **2020**, *57*, 678–696. [CrossRef] [PubMed]
63. Lieu, E.L.; Nguyen, T.; Rhyne, S.; Kim, J. Amino acids in cancer. *Exp. Mol. Med.* **2020**, *52*, 15–30. [CrossRef] [PubMed]
64. Albaugh, V.L.; Pinzon-Guzman, C.; Barbul, A. Arginine metabolism and cancer. *Surg. Oncol. March* **2017**, *115*, 273–280. [CrossRef] [PubMed]

65. Dhama, K.; Karthik, K.; Khandia, R.; Munjal, A.; Tiwari, R.; Rana, R.; Khurana, S.K.; Ullah, S.; Khan, R.U.; Alagawany, M.; et al. Medicinal and therapeutic potential of herbs and plant metabolites/Extracts countering viral pathogens-Current knowledge and future prospects. *Curr. Drug Metab.* **2018**, *19*, 236–263. [CrossRef]
66. Cox-Georgian, D.; Ramadoss, N.; Dona, C.; Basu, C. Therapeutic and medicinal uses of terpenes. In *Medicinal Plants*; Joshee, N., Dhekney, S., Parajuli, P., Eds.; Springer: Cham, Switzerland, 2019; pp. 333–359.
67. Fongang Fotsing, Y.S.; Bankeu Kezetas, J.J. *Terpenoids as important bioactive constituents of essential oils, In Essential oils—Bioactive Compounds, New Perspectives and Application*; Santana de Oliveira, M., Almeida da Costa, W., Gomes Silva, S., Eds.; Intechopen: Rijeka, Croatia, 2020; ISBN 978–1-83962–698–2.
68. Jahangeer, M.; Fatima, R.; Ashiq, M.; Basharat, A.; Qamar, S.A.; Bilal, M.; Iqbal, H.M. Therapeutic and biomedical potentialities of terpenoids–A Review. *J. Pure Appl. Microbiol.* **2021**, *15*, 471–483. [CrossRef]
69. João Matos, M.; Santana, L.; Uriarte, E.; Abreu, O.A.; Molina, E.; Guardado Yordi, E. Coumarins—An important class of phytochemicals in phytochemicals-Isolation. In *Characterisation and Role in Human Health*; Venket Rao, A., Rao, L.G., Eds.; IntechOpen: Rijeka, Croatia, 2015.
70. Küpeli Akkol, E.; Genç, Y.; Karpuz, B.; Sobarzo-Sánchez, E.; Capasso, R. Coumarins and coumarin-related compounds in pharmacotherapy of cancer. *Cancers* **2020**, *12*, 1959. [CrossRef]
71. Kozłowska, A.; Szostak-Węgierek, D. Flavonoids–food sources, health benefits, and mechanisms involved. In *Bioactive Molecules in Food*; Reference Series in Phytochemistry; Mérillon, J.M., Ramawat, K., Eds.; Springer: Cham, Switzerland, 2018.
72. Kozłowska, A.; Szostak-Wegierek, D. Flavonoids-food sources and health benefits. *Rocz. Panstw. Zakl. Hig.* **2014**, *65*, 79–85.
73. Panche, A.N.; Diwan, A.D.; Chandra, S.R. Flavonoids: An overview. *J. Nutr. Sci.* **2016**, *5*, e47. [CrossRef]
74. Kumar, N.; Goel, N. Phenolic acids: Natural versatile molecules with promising therapeutic applications. *Biotechnol Rep.* **2019**, *24*, e00370. [CrossRef]
75. Minatel, I.O.; Vanz Borges, C.; Ferreira, M.I.; Gomez, H.A.G.; Chen, C.Y.O.; Pace Pereira Lima, G. Phenolic compounds: Functional properties, impact of processing and bioavailability. In *Phenolic Compounds-Biological Activity*; Soto-Hernandez, M., Palma-Tenango, M., del Rosario Garcia-Mateos, M., Eds.; IntechOpen: Rijeka, Croatia, 2017.
76. Salehi, B.; Quispe, C.; Sharifi-Rad, J.; Cruz-Martins, N.; Nigam, M.; Mishra, A.P.; Konovalov, D.A.; Orobinskaya, V.; Abu-Reidah, I.M.; Zam, W.; et al. Phytosterols: From preclinical evidence to potential clinical applications. *Front. Pharmacol.* **2021**, *11*, 599959. [CrossRef]
77. Nagy, K.; Tiuca, I.D. Importance of fatty acids in physiopathology of human body. In *Fatty Acids*; Catala, A., Ed.; IntechOpen: Rijeka, Croatia, 2017.
78. Kilcoyne, M.; Joshi, L. Carbohydrates in therapeutics. *Cardiovasc. Hematol. Agents Med. Chem.* **2007**, *5*, 186–197. [CrossRef] [PubMed]
79. Singh, D.; Rajput, A.; Bhatia, A.; Kumar, A.; Kaur, H.; Sharma, P.; Kaur, P.; Singh, S.; Attri, S.; Buttar, H.; et al. Plant-based polysaccharides and their health Functions. *Funct. Foods Health Dis.* **2021**, *11*, 179–200.
80. Hu, X.; Zhang, Y.; Ding, T.; Liu, J.; Zhao, H. Multifunctional gold nanoparticles: A novel nanomaterial for various medical applications and biological activities. *Front. Bioeng. Biotechnol.* **2020**, *8*, 990. [CrossRef] [PubMed]
81. Yeh, Y.C.; Creran, B.; Rotello, V.M. Gold nanoparticles: Preparation, properties, and applications in bionanotechnology. *Nanoscale* **2012**, *4*, 1871–1880. [CrossRef] [PubMed]
82. Siddique, S.; Chow, J.C.L. Gold nanoparticles for drug delivery and cancer therapy. *Appl. Sci.* **2020**, *10*, 3824. [CrossRef]
83. Vega-Vásquez, P.; Mosier, N.S.; Irudayaraj, J. Nanoscale drug delivery systems: From Medicine to Agriculture. *Front. Bioeng. Biotechnol.* **2020**, *8*, 79. [CrossRef]
84. Pala, R.; Anju, V.T.; Dyavaiah, M.; Busi, S.; Nauli, S.M. Nanoparticle-mediated drug delivery for the treatment of cardiovascular diseases. *Int. J. Nanomed.* **2020**, *15*, 3741–3769. [CrossRef]
85. Boomi, P.; Ganesan, R.; Prabu Poorani, G.; Jegatheeswaran, S.; Balakumar, C.; Gurumallesh Prabu, H.; Anand, K.; Marimuthu Prabhu, N.; Jeyakanthan, J.; Saravanan, M. Phyto-engineered gold nanoparticles (AuNPs) with potential antibacterial, antioxidant, and wound healing activities under in vitro and in vivo conditions. *Int. J. Nanomed.* **2020**, *15*, 7553–7568. [CrossRef]
86. Heneczkowski, M.; Kopacz, M.; Nowak, D.; Kuźniar, A. Infrared spectrum analysis of some flavonoids. *Acta Pol. Pharm. Nov.-Dec.* **2001**, *58*, 415–420.
87. Segneanu, A.E.; Marin, C.N.; Ghirlea, I.O.; Feier, C.V.I.; Muntean, C.; Grozescu, I. Artemisia annua Growing Wild in Romania-A metabolite profile approach to target a drug delivery system based on magnetite nanoparticles. *Plants* **2021**, *10*, 2245. [CrossRef]
88. Zhang, Y.C.; Deng, J.; Lin, X.L.; Li, Y.M.; Sheng, H.X.; Xia, B.H.; Lin, L.M. Use of ATR-FTIR spectroscopy and chemometrics for the variation of active components in different harvesting periods of Lonicera japonica. *Int. J. Anal. Chem.* **2022**, *2022*, 8850914. [CrossRef] [PubMed]
89. Mabasa, X.E.; Mathomu, L.M.; Madala, N.E.; Musie, E.M.; Sigidi, M.T. Molecular spectroscopic (FTIR and UV-Vis) and hyphenated chromatographic (UHPLC-qTOF-MS) analysis and in vitro bioactivities of the Momordica balsamina leaf extract. *Biochem. Res. Int.* **2021**, *2021*, 2854217. [CrossRef] [PubMed]
90. Scarsini, M.; Thurotte, A.; Veidl, B.; Amiard, F.; Niepceron, F.; Badawi, M.; Lagarde, F.; Schoefs, B.; Marchand, J. Metabolite quantification by Fourier Transform Infrared Spectroscopy in diatoms: Proof of concept on Phaeodactylum tricornutum. *Front. Plant. Sci.* **2021**, *12*, 756421. [CrossRef]

91. Topală, C.M.; Tătarua, L.D.; Ducu, C. ATR-FTIR spectra fingerprinting of medicinal herbs extracts prepared using microwave extraction. *Arab. J. Med. Aromat. Plants AJMAP* **2017**, *3*, 1–9.
92. Seuvre, A.M.; Mathlouthi, M. FT-IR. spectra of oligo- and poly-nucleotides. *Carbohydr. Res.* **1987**, *169*, 83–103. [CrossRef]
93. Umashankar, T.; Govindappa, M.; Ramachandra, Y.L.; Rai, P.; Channabasava, S. Isolation and characterization of coumarin isolated from endophyte, Alternaria species-1 of *Crotalaria pallida* and its apoptotic action on HeLa cancer cell line. *Metabolomics* **2015**, *5*, 158.
94. Salem, M.; Marzouk, M.; El-Kazak, A. Synthesis and characterization of some new coumarins with in vitro antitumor and antioxidant activity and high protective effects against DNA damage. *Molecules* **2016**, *21*, 249. [CrossRef]
95. Baranska, M.; Schulz, H. Chapter 4 Determination of alkaloids through Infrared and Raman Spectroscopy. *Alkaloids Chem. Biol.* **2009**, *67*, 217–255.
96. Pang, M.; Jiang, S.; Cao, L.; Pan, L. Novel synthesis of steryl esters from phytosterols and amino acid. *J. Agric. Food Chem.* **2011**, *59*, 10732–10736. [CrossRef]
97. Thottoli, A.K.; Unni, A.K.A. Effect of trisodium citrate concentration on the particle growth of ZnS nanoparticles. *J. Nanostructure Chem.* **2013**, *3*, 56. [CrossRef]
98. Tao, C. Antimicrobial activity and toxicity of gold nanoparticles: Research progress, challenges and prospects. *Lett Appl Microbiol.* **2018**, *67*, 537–543. [CrossRef] [PubMed]
99. Hitaishi, V.P.; Mazurenko, I.; Vengasseril Murali, A.; de Poulpiquet, A.; Coustillier, G.; Delaporte, P.; Lojou, E. Nanosecond laser–fabricated monolayer of gold nanoparticles on ITO for bioelectrocatalysis. *Front. Chem.* **2020**, *8*, 431. [CrossRef] [PubMed]